The preparation of CuInSe$_2$ films by solvothermal route and non-vacuum spin-coating process

Paifeng Luo*, Penghan Yu, Ruzhong Zuo, Jiao Jin, Yuankui Ding, Junda Song, Yutong Chen

Department of Materials Science and Engineering, Hefei University of Technology, Hefei, Anhui 230009, PR China

ABSTRACT

A low-cost non-vacuum process for fabrication of CuInSe$_2$ (CIS) films by a solvothermal route and spin-coating method is described. First, the CIS precursor powders are synthesized by solvothermal technology. Second, the CIS films are deposited via spin-coating from precursor slurry consisting of CIS particles and selenization process. Through X-ray diffraction (XRD), scanning electron microscopy (SEM), energy dispersive X-ray spectroscopy (EDS) and absorption spectroscopy measurement, the CIS nanoparticle precursors consisted mainly of plate-like particles showing the chalcopyrite structure with preferred (1 1 2) orientation. Typical near stoichiometric single phase CIS films with a micron-sized dense grains are prepared after selenization process. An energy band gap about 1.02 eV and an absorption coefficient exceeding 10^5 cm^{-1} are also obtained in our work.

© 2010 Elsevier B.V. All rights reserved.

1. Introduction

CIS and related materials, which are characterized by a suitable band gap, a high absorption coefficient and good stability, have been leading thin-film material candidates for incorporation in high-efficiency photovoltaic devices [1–4]. Various processing techniques, which include co-evaporation [5], sputtering [6,7] and pulsed laser deposition (PLD) [8–10] have been used for preparation of high quality CIS thin films. However, conventional vacuum methods have drawbacks such as complexity in process, high production costs and difficulty in scaling up, which are to be solved before the commercialization of the CIS solar cells. On the other hand, the low-cost non-vacuum techniques for CIS deposition are inherently suitable for large-scale applications and benefit from established industries of coatings, paints, inks, electronic ceramics and colloidal systems.Many alternative non-vacuum coating techniques have been proposed and investigated for the deposition of CIS absorber layer. Kapur et al. [11] and Eberspacher et al. [12] have obtained high efficiencies of 13.6% and 11.7% using metal oxide precursors followed by a reduction and selenization process, respectively. However, there are several drawbacks while using metal oxides as precursor materials for CIS solar cells. First, the use of oxide-based particles in CIS absorber layer construction requires a high-temperature hydrogen reduction step to reduce the oxides. In addition to requiring substantial time and energy, this step is potentially explosive. Second, the

mechanical milling may result in the non-uniform distribution of the particle size and increase the cost. Further, it is very difficult to effectively incorporate gallium into a nascent copper indium precursor film using a metal oxide synthesis approach. Thus, there is a need in the art, for a non-oxide, nanoparticle based precursor material which could overcome the above disadvantages.

Concerning the fabrication technique of nanoparticle, solvothermal method has the advantage of being a simple and inexpensive low-temperature process, which does not require organometallic or toxic precursors. Jiang et al. [13], Li et al. [14] and Chun et al. [15] have reported that the CIS and CuInGaSe$_2$ (CIGS) particles can be obtained by the solvothermal route. But the high quality CIS films from the CIS nanoparticle precursors by the solvothermal route are little reported. So a potential method for non-vacuum CIS precursor formation is developed in our work. First, the CIS precursor powders are synthesized by the solvothermal technology. Second, the CIS films are deposited via spin-coating from precursor slurry consisting of CIS particles and selenization process. The structure and the optical properties of the CIS nanoparticle precursors and the CIS films are also investigated.

2. Experimental

Fig. 1 shows the schematic diagram of CIS films fabrication with non-vacuum process. First, the CIS nanoparticle precursors are synthesized by the solvothermal route. In a typical synthesis, the required amount of CuCl$_2$·2H$_2$O (0.221 g), InCl$_3$·4H$_2$O (0.381 g) and Se (0.204 g) powders are loaded into a 50 ml

* Corresponding author. Tel.: +86 551 2904566; fax: +86 551 2905285.
E-mail address: lpfeng@mail.ustc.edu.cn (P. Yu).

Teflon lined autoclave, which is then filled with anhydrous ethylenediamine up to 80% of the total volume. The sealed autoclave is maintained at a reaction temperature 180 °C for 18 h and then allowed to cool to room temperature. The precipitate is centrifuged and washed with distilled water and ethanol several times. The particles are filtered off and dried at 60 °C for 6 h and milled at ambient temperature in an agate mortar for 3 h. Second, suitable thickening agents ethyl cellulose and dispersant polyethylene glycol are selected to formulate the slurry with suitable viscosity. The CIS precursor layers are deposited via spin-coating from precursor slurry. The sample is heated to remove the solvent and burn organic additive. Subsequently, the pretreatment films are selenized in a two-zone furnace with a quasi-closed quartz crucible under a vacuum furnace of 3×10^{-2} Pa in order to get dense CIS absorber layers. Fig. 2 shows the schematic diagram of a two-zone furnace for selenization. In order to avoid oxygen, we used argon for washing the chamber for three times. The selenization treatment is performed at 500 °C for 1 h with Se vapor evaporated at 300 °C and is carried out by Ar.

Phase composition and crystal structure of films are identified by the XRD method (D/Max-rA). The morphology of films is observed on a field emission scanning electron microscope (FESEM, JEOL-JSM-6700F). The composition of CIS films is also measured by the SEM-EDS. The optical absorption spectrum is recorded on a UV–vis-365-type spectrophotometer in a range 800–1500 nm.
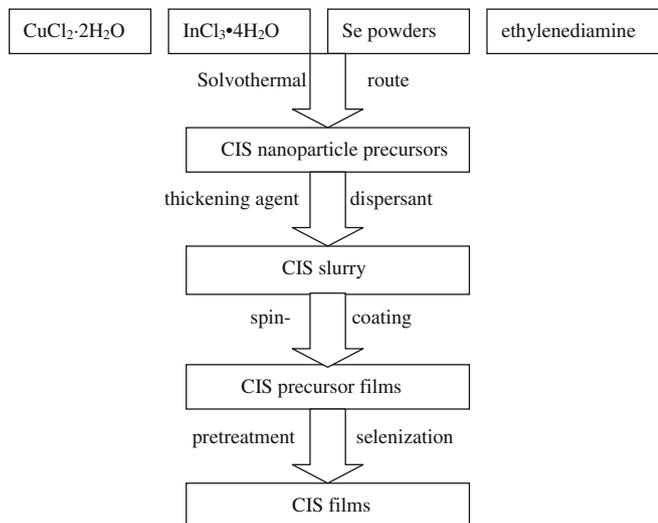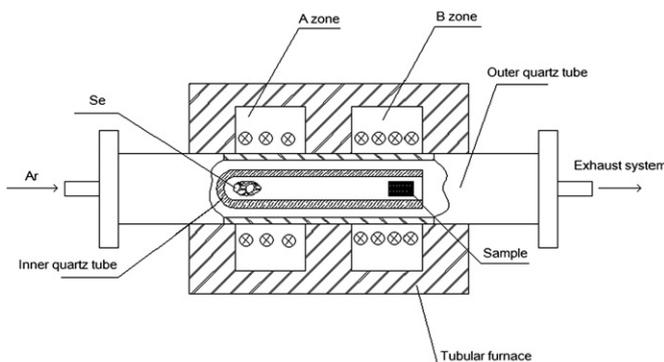
3. Results and discussions

Fig. 3 shows the X-ray diffraction patterns of the CIS nanoparticle precursors and CIS films. The CIS nanoparticle precursors prepared by the solvothermal route exhibit preferential orientation along the chalcopyrite phase α-CIS (1 1 2) direction at 26.6°, as shown in Fig. 3(a). The other prominent peaks observed correspond to the (2 0 4)/(2 2 0) and (1 1 6)/(3 1 2) phases. All peaks observed on the patterns are well accord with the diffraction lines in the chalcopyrite structure of CIS, except the secondary $Cu_{2-x}Se$ phase. After selenization, as shown in Fig. 3(b), the intensity ratio of the (1 1 2) peak to the (2 0 4)/(2 2 0) peak exceeds three times indicating that there is a deep degree of (1 1 2) preferred orientation in this film. In addition to these commonly observed orientations, the weak orientations such as (1 0 3), (2 1 1) and (0 0 8) are also observed in the XRD pattern, distinguishing the chalcopyrite phase from the sphalerite phase [14]. The presence of these peaks clearly indicates the perfect chalcopyrite structure. The secondary $Cu_{2-x}Se$ phase disappeared and converted to pure chalcopyrite product by selenization at 500 °C, which is in good agreement with the experimental phenomenon reported by Olejnicek et al. [16].
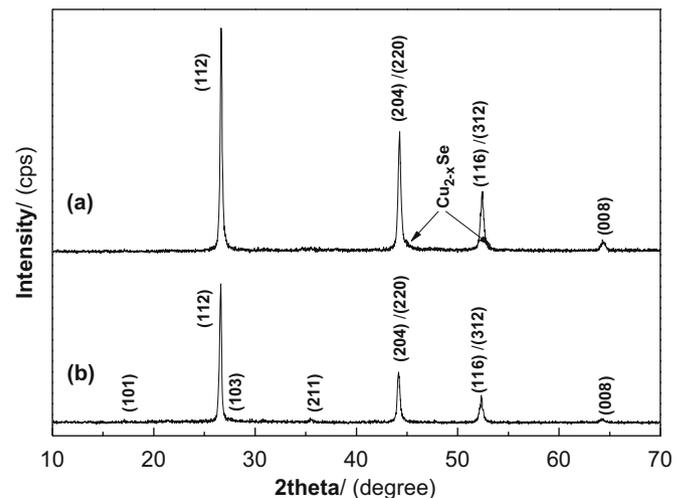

Fig. 1. The schematic diagram of CIS films fabrication with non-vacuum process.

Fig. 2. The schematic diagram of a two-zone furnace for selenization.

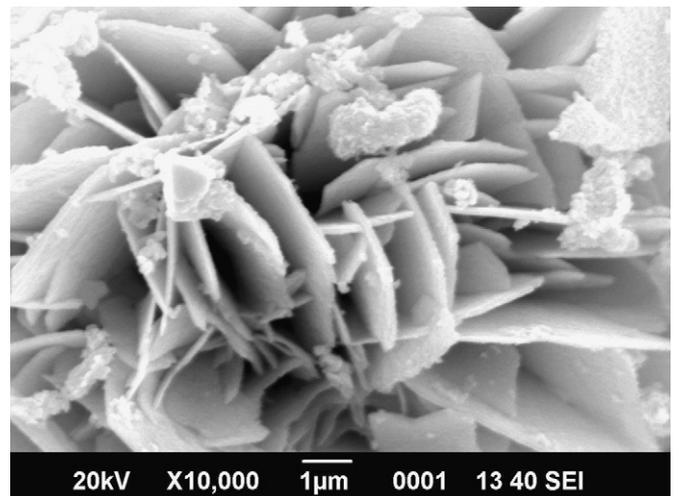**Fig. 3.** The XRD pattern of the CIS nanoparticle precursors and CIS films.

Fig. 4. The planar SEM micrograph of the CIS nanoparticle precursors.

Fig. 4 shows the planar SEM micrograph of the CIS nanoparticle precursors. A large number of plate-like particles are obtained from the reaction in ethylenediamine and little anomalistic particles are also observed in the SEM picture. The enlarged image is shown in Fig. 5. Chun et al. [15] insist that it can be explained by the solutin–liquid–solid (SLS) mechanism for the one-dimensional growth suggested by Trentler et al. [17]. In the SLS mechanism, the presence of the liquid phase is a very important parameter. For the reaction temperature lower than that of the melting point of indium, the coverage of the liquid phase on the solid phase could be relatively low, which could result in plate-like particles. On the other hand, full coverage of the liquid phase on the solid phase could result in spherical particles. In fact, we can also obtain the plate-like particles at 180 °C, which is above the melting point of indium. So it can be concluded that the reaction mechanism should be more studied.

Figs. 6 and 7 show the planar and the cross-sectional SEM micrograph of the CIS precursor films, respectively. After milling and spin-coating, particles with size distribution of 200–5000 nm, and mixture of various shaped particles (spherical+triangular+plate-like, etc.) are obtained. Generally, particles of different sizes will lead to different melting temperatures. The uniform CIS particles, which would be the key to homogeneous dense CIS films are obtained in our work. Figs. 8 and 9 show the planar and the cross-sectional SEM micrograph of the CIS films, respectively. The CIS precursor particles grow up to micrometers after selenizaton process at 500 °C for 1 h. The dense and the
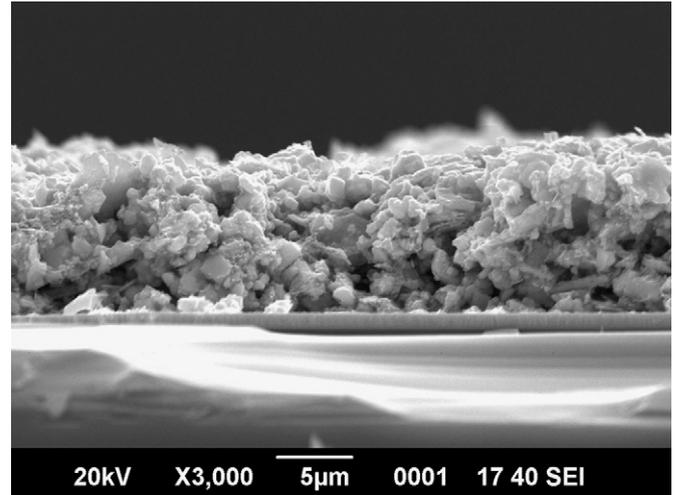

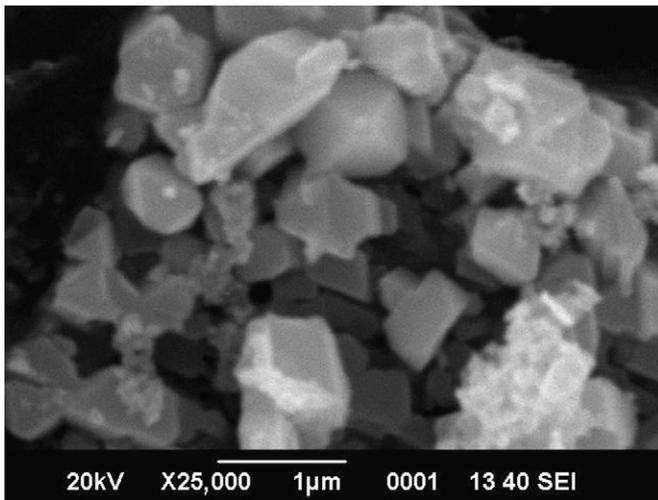**Fig. 7.** The cross-sectional SEM micrograph of the CIS precursor films.

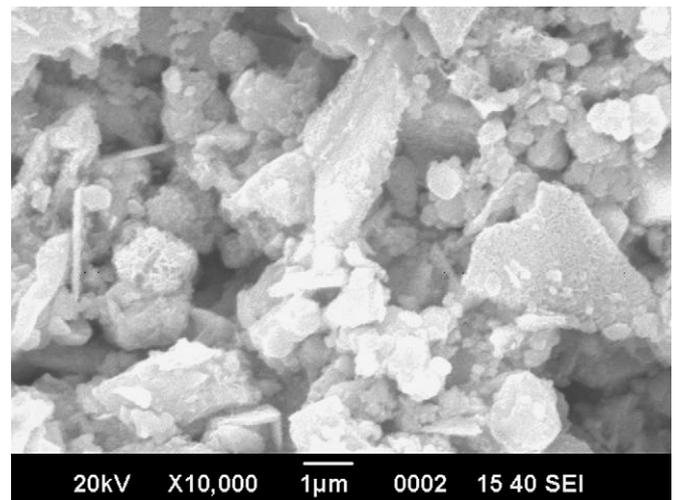**Fig. 5.** The enlarged SEM image of the CIS nanoparticle precursors.
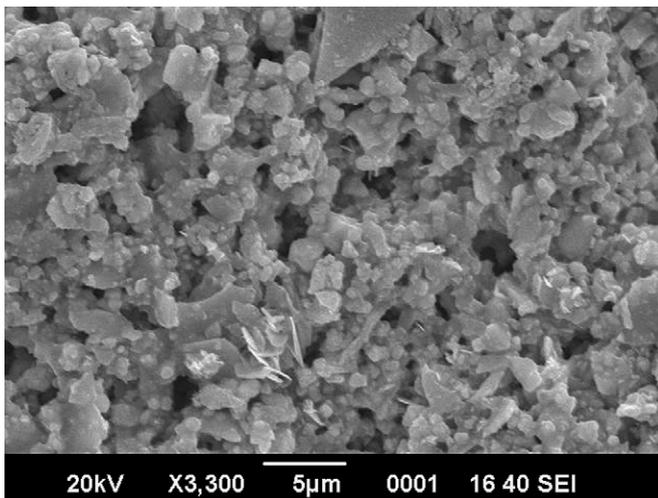

Fig. 8. The planar SEM micrograph of the CIS films.

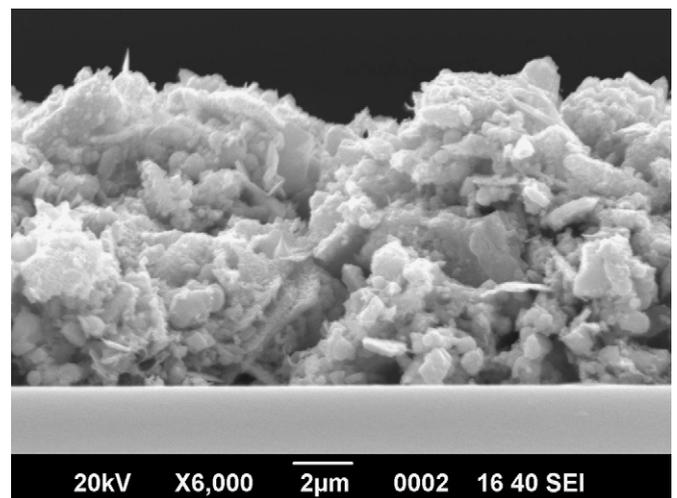**Fig. 6.** The planar SEM micrograph of the CIS precursor films.

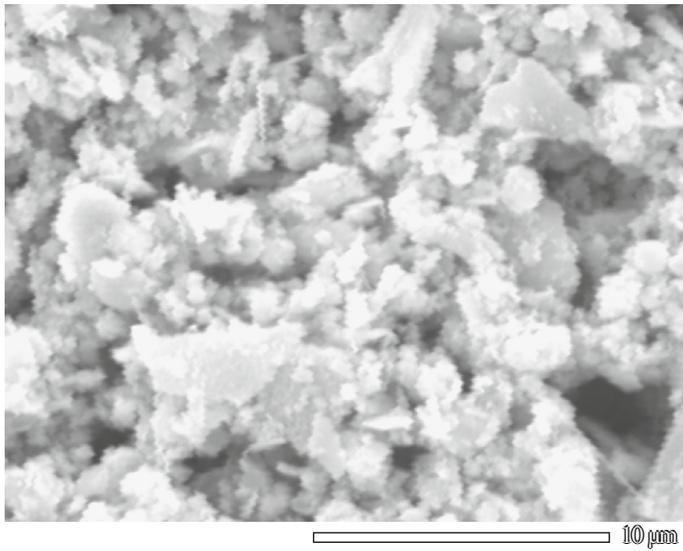**Fig. 9.** The cross-sectional SEM micrograph of the CIS films.

Fig. 10. The composition of the CIS nanoparticle precursors determined by the EDS.
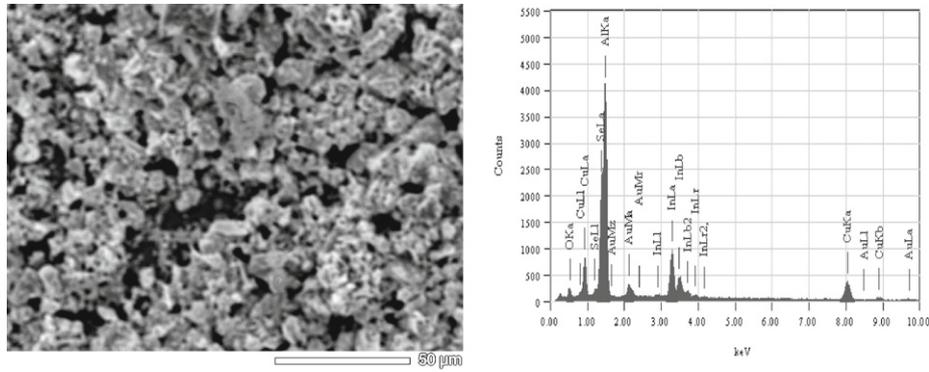
Name	Cu%	In%	Se%
Ar.%	19.79	19.69	32.87

Name	Cu%	In%	Se%
Ar.%	16.87	17.03	33.86

Fig. 11. The composition of the CIS films determined by EDS.

well-defined uniform grains with large size that attained micron levels are formed. The photovoltaic devices are typically fabricated using a uniform absorber layer applied in solar cells in order to avoid the formation of undesirable shunt paths. So according to the experiment result, the CIS films with micron-sized dense grains are obtained after selenization process.

The compositions of the CIS nanoparticle precursors and the CIS films are determined by EDS, as shown in Figs. 10 and 11. The ratio of Cu/In/Se(19.79:19.69:32.87) in the CIS nanoparticle precursors is close to 1/1/1.7, which is obviously inconsistent with the stoichiometric ratio and shows a Se-poor film. This is probably due to the existence of the secondary phase $Cu_{2-x}Se$ and is also very consistent with the XRD result. After selenization process, the ratio of Cu/In/Se(16.87:17.03:33.86) is close in composition to 1/1/2. A typical near stoichiometric CIS film is obtained in our work. Moreover, many impurities, such as C, O and Au, are also detected. The elements C and O cannot be avoided and the element Au is due to the introduction of electron microscopy experiments, the process of steaming golden.
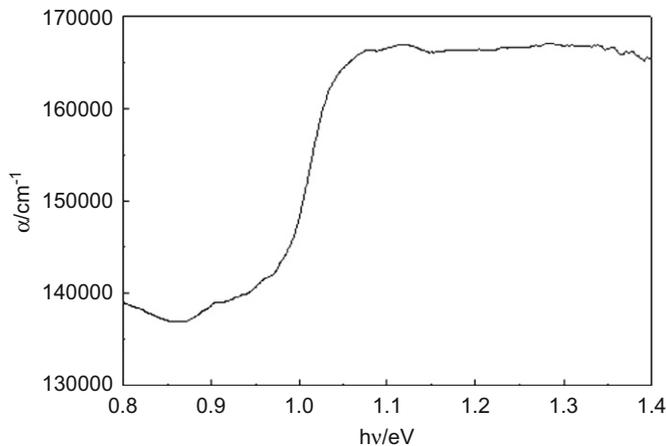
Fig. 12. The photon energy dependence of the absorption coefficient for CIS films.

The optical absorption spectra are recorded on a UV–vis-365-type spectrophotometer in a range 800–1500 nm. Fig. 12 shows the photon energy dependence of the absorption coefficient for CIS films. An absorption coefficient exceeding 10^5 cm^{-1} is obtained by absorption spectroscopy measurement, which shows a good optical quality of the films. As we all know, CIS is a direct-gap semiconductor with a maximum valence-band and a minimum conduction-band at $k=0$. So an energy band gap about 1.02 eV is obtained by absorption spectroscopy measurement, which is obtained by the calculation of the midpoint of the absorption edge wavelength $\lambda = 1220$ nm. The energy band gap is almost identical with the theoretical standard value of CIS films at room temperature [18].

4. Conclusion

The single chalcopyrite phase CIS films are successfully prepared by a low-cost non-vacuum process. The nanoparticle precursors consisted mainly of plate-like particles by the solvothermal route which shows the chalcopyrite structure with preferred (1 1 2) orientation. After milling, spin-coating and selenization process, the typical near stoichiometric CIS films with a micron-sized dense grains are prepared. An energy band gap about 1.02 eV and an absorption coefficient exceeding

10^5 cm^{-1} are also determined by the absorption spectroscopy measurement. In a word, this paper reports a low-cost non-vacuum process for synthesizing CIS films by using the solvothermal route and the spin-coating technology, which indicates a promising way for the application in solar cells.

References

[1] J. Guillemoles, U. Rau, L. Kronik, H. Schock, D. Cahen, Adv. Mater. 11 (1999) 957.
[2] K. Ramanathan, M.A. Contreras, C.L. Perkins, S. Asher, F.S. Hasoon, J. Keane D. Young, M. Romero, W. Metzger, R. Noufi, J. Ward, A. Duda, Prog. Photovolt.: Res. Appl. 11 (2003) 225.
[3] Q.J. Guo, S.J. Kim, M. Kar, W.N. Shafarman, R.W. Birkmire, E.A. Stach R. Agrawal, H.W. Hillhouse, Nano Lett. 8 (2008) 2982.
[4] R. Yanfa Yan, Noufi, M.M. Al-Jassim, Phys. Rev. Lett. 96 (2006) 205501.
[5] M.A. Contreras, B. Egaas, K. Ramanathan, J. Hiltner, A. Swartzlander F. Hasoon, R. Noufi, Prog. Photovolt.: Res. Appl. 7 (1999) 311.
[6] J.Y. Zhang, X.B. Gong, W.Y. Liu, Y.M. Xue, F.Y. Li, Z.Q. Zhou, Y. Sun, C.J. Li Z.L. Sun, Acta Energiae Solaris Sin. 24 (2003) 335.
[7] Jiayou Fangdan Jiang, Thin Solid Films 515 (2006) 1950.
[8] A. Yoshida, N. Tanahashi, T. Tanaka, Y. Demizu, Y. Yamamoto, T. Yamaguchi, Sol. Energy Mater. Sol. Cells 50 (1998) 7.
[9] P. Victor, J. Nagaraju, S.B. Krupanidhi, Solid State Commun. 116 (2000) 649.
[10] P.F. Luo, C.F. Zhu, G.S. Jiang, Solid State Commun. 146 (2008) 57.
[11] V.K. Kapur, A. Bansal, P. Le, O.I. Asensio, Thin Solid Films 53 (2003) 431–432.
[12] C. Eberspacher, K. Pauls, J. Serra, Non-vacuum processing of CIGS solar cells, in: Photovoltaic Specialists Conference, Conference Records of the 29th IEEE PVSEC, New Orleans, USA, 2002, p. 684.
[13] Y. Jiang, Y. Wu, X. Mo, W. Yu, Y. Xie, Y. Qian, Inorg. Chem. 39 (2000) 2964.
[14] B. Li, Y. Xie, J. Huang, Y. Qian, Adv. Mater. 11 (1999) 1456.
[15] Y.-G. Chun, K.-H. Kim, K.-H. Yoon, Thin Solid Films 480 (2005) 46.
[16] J. Olejnicek, C.A. Kamler, A. Mirasano, A.L. Martinez-Skinner, M.A. Ingersoll, C.L. Exstrom, S.A. Darveau, J.L. Huguenin-Love, M. Diaz, N.J. Ianno, R.J. Soukup, Sol. Energy Mater. Sol. Cells 94 (2010) 8.
[17] T.J. Trentler, K.M. Hickman, S.C. Goel, A.M. Viano, P.C. Gibbons, W.E. Buhro, Science 207 (1995) 1791.
[18] H.S. Soliman, M.M. Elnahas, O. Jamjoum, Kh.A. Mady, J. Mater. Sci. 23 (1988) 4071.